

Robust synchronization of spin-torque oscillators with an LCR load

Arkady Pikovsky

Department of Physics and Astronomy, Potsdam University,

Karl-Liebknecht-Str 24, D-14476, Potsdam, Germany and

NEXT, Laboratoire de Physique Théorique du CNRS,

IRSAMC, Université Toulouse, UPS, 31062 Toulouse, France

(Dated: August 3, 2021)

Abstract

We study dynamics of a serial array of spin-torque-oscillators with a parallel inductor-capacitor-resistor (LCR) load. In a large range of parameters the fully synchronous regime, where all the oscillators have the same state and the output field is maximal, is shown to be stable. However, not always such a robust complete synchronization develops from the random initial state, in many cases nontrivial clustering is observed, with a partial synchronization resulting in a quasiperiodic or chaotic mean field dynamics.

PACS numbers: 05.45.Xt, 85.75.-d

I. INTRODUCTION

Spin-torque oscillator (STO) is a nanoscale spintronic device generating periodic microwave (in the frequency range of several GHz) oscillations (see¹ for an introductory review). The physics behind these oscillations is based on the spin-transfer torque force, with which a spin-polarized electrical current acts on a free magnet. Sometimes one uses terms “Spin-transfer oscillator” or “Spin-transfer nano-oscillator” (STNO) to describe this object. The STO consists of two magnetic layers, one (bottom) having fixed magnetization \vec{M}_0 is relatively thick, and the other (top) with free, precessing magnetization \vec{M} , is relatively thin. These layers are separated by a non-magnetic spacer. Characteristic widths of 100 nm allow to describe STO as a nano-device. If the current (in vertical direction) is applied, then when passing the fixed layer, the spin directions of the electrons align to the direction of \vec{M}_0 . As these electrons enter the free layer, a spin transfer torque acts on its magnetization \vec{M} , tending to reorient it, as has been theoretically predicted by Slonczewski² and Berger³. As has been realized by Slonczewski², the spin transfer torque can compensate the damping of the spin precession of the free layer, and in a constant external magnetic field a sustained oscillation (rotation of vector \vec{M}) is observed.

After experimental observation of the generation^{4,5}, a lot of attention has been recently attracted to synchronization of STOs. Indeed, as self-sustained oscillators like electronic generators and lasers, they must demonstrate typical for this class of physical systems effects of phase locking by external injection, and of mutual synchronization if two or more devices are coupled⁶. Beside from the fundamental interest, synchronization of STOs is also of high practical relevance, as a way to increase the output power of otherwise rather weak individual STOs⁷.

In the context of uniform STOs, the mostly promising way of coupling the STOs to achieve synchrony is to connect them in serial electrically via the common microwave current^{8–12} (in experiments^{13,14} a synchronization of two STOs was observed; however the coupling was not the electrical one, but due to spin waves, as the distance between two STOs build on the same mesa was about 500 nm). In Ref.⁸ a prototype model for such a coupling has been suggested, where N STOs are connected in series and are subject to a common dc current, with a parallel resistive load. The coupling is due to the giant magnetic resistance (GMR) effect, as the resistance of an STO R_i depends on the orientation of its magnetization \vec{M}_i ,

so that the redistribution of the ac current between the STO array and the load depends on the the average (over the ensemble of N STOs) value of this resistance $\langle R_i \rangle$. This situation is a typical mean-field coupling of oscillators, mostly prominent exemplified by the Kuramoto model^{15,16}. This setup has been further studied in^{11,12}, with a more emphasis on nonlinear dynamical description of the ensemble behavior. The result of these studies is that synchronization is very hard to achieve, and if it is observed, it is rather sensitive and not robust. Also further numerical simulations^{10,11} have shown a large variety of multistable regimes including non-synchronized states. These observations have been recently confirmed by the analysis of two coupled STOs¹².

Another approach to study synchronization properties of STOs, based not on the exact microscopic equations (Eqs. (2) below), but on general equations for self-sustained oscillators has been proposed in^{1,17} and followed in^{9,18,19}. Because here the resulting dynamics is only suggested based on general qualitative arguments, but not derived from the microscopic equations, predictions for synchronization properties do not extend beyond standard qualitative ones. In particular, in this approach one writes an effective Kuramoto-type model for many mutually coupled STOs⁹, which does not represent the sensitivity observed in the simulation based on the microscopic equations.

In this paper we study theoretically a serial array of STOs subject to a dc current, with a general parallel inductor-capacitor-resistor (LCR) load. This setup is highly motivated by similar studies of synchronization of Josephson junctions^{20,21}. In particular, in²² such a model has been directly compared to the experiments with Josephson junctions in a strongly resonant cavity²³. The LCR load can operate, depending on the frequency, either as an inductive one, or as a capacitive one. This flexibility allows one to find, similar to the case of Josephson junctions, situations with a robust synchronization of STOs. We show also, that transition to synchrony as the parameter (dc current) varies, occurs through rather complex states of partial synchrony and clustering, not presented in the standard Kuramoto model.

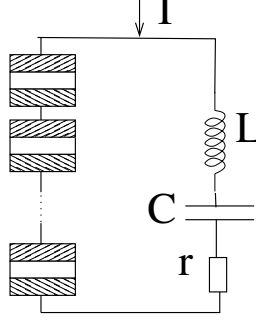


FIG. 1. The equivalent circuit of the serial array of STO oscillators with a LCR load.

II. BASIC MODEL

We consider an array of STOs with a LCR load as depicted in Fig. 1. The equations for the load are

$$LC \frac{d^2 V}{dt^2} + rC \frac{dV}{dt} + V = R(I - C \frac{dV}{dt}), \quad (1)$$

where R is the time-dependent resistance of the STO array, which is subject to current $J = I - C \frac{dV}{dt}$. Eq. (1) is complemented by the system of equations for STOs.

Each STO is described by its free-layer magnetization \vec{M}_i which obeys the Landau-Lifshitz-Gilbert-Slonczewski equation

$$\frac{d}{dt} \vec{M}_i = -\gamma \vec{M}_i \times \vec{H}_{eff} + \alpha \vec{M}_i \times \frac{d}{dt} \vec{M}_i + \gamma \beta J \vec{M}_i \times (\vec{M}_i \times \vec{M}_0), \quad (2)$$

where γ is the gyromagnetic ratio; α is the Gilbert damping constant; β contains material parameters; J is the current through the STO; the effective magnetic field \vec{H}_{eff} contains an external magnetic field, an easy-axis field, and an easy-plane anisotropy field; \vec{M}_0 is magnetization of the fixed layer.

Following¹⁰ we assume that $\vec{H}_{eff} = H_a \hat{e}_x + (H_k M_x \hat{e}_x - H_{dz} M_z \hat{e}_z) / |\vec{M}|$. Then, in spherical coordinates (ϕ, θ) the LLGS equations read¹⁰

$$\begin{aligned} \frac{1 + \alpha^2}{\gamma} \dot{\theta}_i &= U \cos \theta_i \cos \phi_i - W \sin \phi_i + \alpha S - T, \\ \frac{1 + \alpha^2}{\gamma} \sin \theta_i \dot{\phi}_i &= -U \sin \phi_i - W \cos \phi_i \cos \theta_i - S - \alpha T, \end{aligned} \quad (3)$$

where

$$\begin{aligned} S &= (H_{dz} + H_k \cos^2 \phi_i) \sin \theta_i \cos \theta_i, & T &= H_k \sin \phi_i \cos \phi_i \sin \theta_i, \\ U &= \alpha H_a - \beta J, & W &= H_a + \alpha \beta J. \end{aligned} \quad (4)$$

The system is closed by relating the resistance of the array R to the states of the STOs ϕ_i, θ_i . According to Ref.⁸, the resistance depends on the angle δ between the magnetizations in the fixed and the free layers. In our case the magnetization of the fixed layer is along x -axis, therefore $\cos \delta = \sin \theta \cos \phi$. It is assumed that the resistance varies between value R_P (parallel magnetizations, $\delta = 0$) and R_{AP} (antiparallel magnetizations, $\delta = \pi$) according to

$$F(\theta, \phi) = \frac{R_P + R_{AP}}{2} - \frac{R_{AP} - R_P}{2} \cos \delta = R_0 - R_1 \sin \theta \cos \phi ,$$

where $R_0 = \frac{R_P + R_{AP}}{2}$ and $R_1 = \frac{R_{AP} - R_P}{2}$. Then we calculate R :

$$R = \sum_1^N (R_0 - R_1 \sin \theta \cos \phi) = \rho(1 - \varepsilon X) , \quad (5)$$

where

$$\rho = NR_0 , \quad \varepsilon = \frac{R_1}{R_0} , \quad X = \langle \sin \theta \cos \phi \rangle = \frac{1}{N} \sum_1^N \sin \theta_i \cos \phi_i . \quad (6)$$

The final system of equations is a combination of Eqs. (1,3,4,5,6). We write it the dimensionless form, for the derivation we refer to the Appendix A:

$$\begin{aligned} \frac{d\theta_i}{dt} &= U \cos \theta_i \cos \phi_i - W \sin \phi_i + \alpha S - T , \\ \sin \theta_i \frac{d\phi_i}{dt} &= -U \sin \phi_i - W \cos \phi_i \cos \theta_i - S - \alpha T , \\ \frac{du}{dt} &= \frac{\omega}{N} w , \\ \frac{dw}{dt} &= \frac{N\Omega^2}{\omega} [(1 - \varepsilon X)(1 - w) - u] , \\ S &= (H_{dz} + H_k \cos^2 \phi_i) \sin \theta_i \cos \theta_i , \quad T = H_k \sin \phi_i \cos \phi_i \sin \theta_i , \\ U &= \alpha H_a - \beta I(1 - w) , \quad W = H_a + \alpha \beta I(1 - w) , \\ X &= \frac{1}{N} \sum_1^N \sin \theta_i \cos \phi_i . \end{aligned} \quad (7)$$

Here variables θ_i, ϕ_i describe individual STOs in the array, $u \sim V$ and $w \sim \frac{dV}{dt}$ are global variables describing the load, and the interaction between these systems is via the mean field X .

Below we fix parameters of the STOs following Ref.¹⁰

$$H_a = 0.2 , \quad \alpha = 0.01 , \quad \beta = \frac{10}{3} , \quad H_{dz} = 1.6 , \quad H_k = 0.05 ,$$

focusing on the dependence on the dimensionless parameters of the load Ω, ω , the coupling parameter ε , and on the external current I .

III. DYNAMICAL STATES

In the ensembles of globally coupled identical oscillators, different dynamical regimes are generally possible:

- Complete synchrony, where states of all oscillators coincide, and coincide also with the mean fields. The dynamics reduces then to a low-dimensional system that includes the oscillator variables and the global fields (in our case the variable of the load). This regime is the mostly interesting one from the applied viewpoint, as here all the individual fields are summed coherently and the output field is maximal. It is, however, mostly boring from the dynamical viewpoint.
- Clustered state, where oscillators form several clusters, within each of them their states coincide. Complete synchrony can be considered as the 1-cluster state; typically prevail states with a small number of clusters, but sometimes several clusters coexist with dispersed oscillators not belonging to clusters. Clustering means strong reduction of the number of independent variables, but the resulting regime can be quite complex as the dimension of the total system is larger than one in the case of complete synchrony.
- Asynchronous state, where all the oscillators remain different, and the mean field that mediates the interaction vanishes: one has in fact an ensemble of practically non-interacting elements.
- Partial synchronization, where the oscillators remain different but the mean fields do not vanish, and have macroscopic (compared with the finite-size fluctuations) values. These regimes are mostly difficult to describe, and a good theory exists in exceptional cases only^{24,25}. The dynamics of the mean fields may be periodic^{24–26} or chaotic^{27,28}.

Remarkably, for the considered array of STOs, we observe all these possible states, as described below. In Fig. 2 we show the dependence of the averaged over the time variation mean field $\text{var}(X) = \overline{(X(t) - \bar{X})^2}$ in dependence on the external current I , for $\omega = 1$, $\Omega = 0.5$, $\varepsilon = 0.3$, $N = 200$. To check for a possible multistability, for each set of parameters different runs starting from random initial conditions have been performed, and the values in each runs are shown with a marker. Thus vertical spreading of markers indicates for multistability; it is mostly pronounced for $0.006 \lesssim I \lesssim 0.0085$, here clusters with different

distributions are formed. For $0.0085 \gtrsim I$ one observes a complete synchrony, for $I \gtrsim 0.0045$ an asynchronous state occurs, and for $0.0045 \gtrsim I \gtrsim 0.006$ a partial synchrony is observed. We describe these regimes in details below, using the same parameters as in Fig. 2.

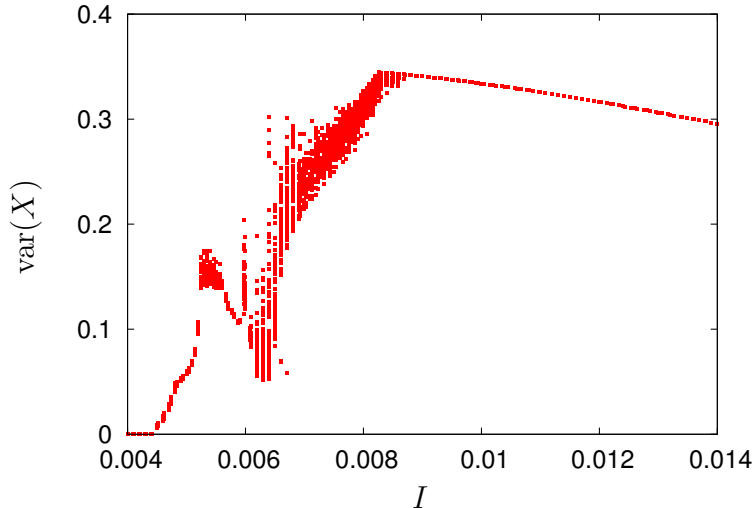


FIG. 2. Variation of the mean field for $\Omega = 0.5$, $\varepsilon = 0.3$, $\omega = 1$, $N = 200$ in dependence on the current I . The time averaging has been performed over time interval 10^5 .

A. Complete synchrony and its stability

For a set of identical oscillators, the fully synchronous state usually means that all the dynamical variables of the array coincide. Here, because of symmetry $\theta, \phi \rightarrow \pi - \theta, -\phi$, the variables θ_i, ϕ_i do not necessarily coincide, therefore we introduce observables $x_i = \sin \theta_i \cos \phi_i$, $y_i = \cos \theta_i \sin \phi_i$ that are not affected by the symmetry transformation. An additional advantage is that the mean field is just the average of x_i : $X = \frac{1}{N} \sum x_i$. Unfortunately, rewriting equations in these variables appears not possible, so we use them as “observables” to illustrate the dynamics, while performing calculations in the variables θ, ϕ .

In the fully synchronous regime system (7) is a four-dimensional dissipative driven system of ODEs which in a large range of parameters possess a stable periodic (with period T) solution $(\theta^0(t), \phi^0(t), u^0(t), w^0(t))$ describing STO oscillations. Depending on parameters, this limit cycle passes through a homoclinic bifurcation, at which its period becomes infinite, and the topology of the cycle on the sphere (ϕ, θ) changes (which is clearly seen in Fig. 3(b) as the transition from a “small” to a “large” cycle). We illustrate this in Fig. 3, where we

show the cycle in the introduced coordinates x, y , and also in the stereographic projection.

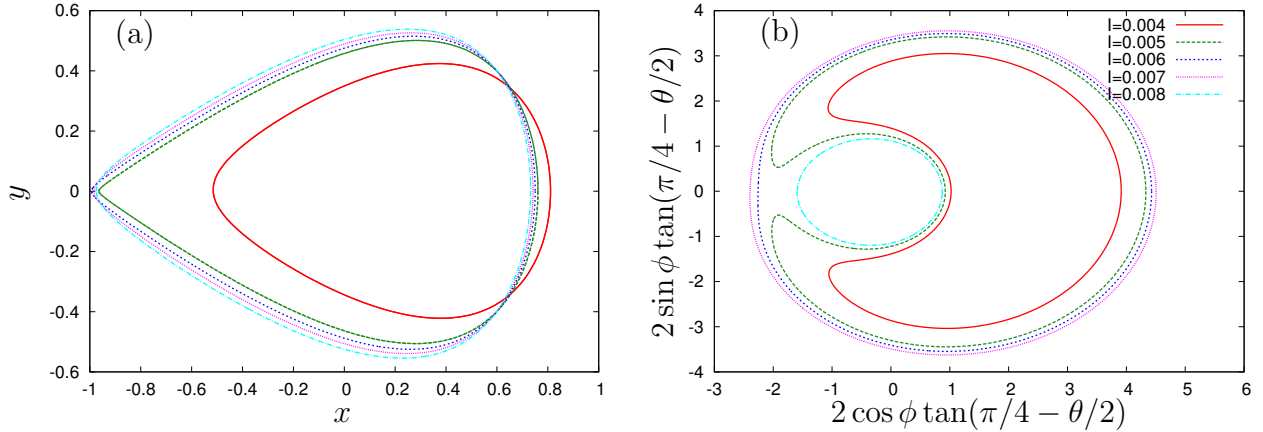


FIG. 3. (color online) Synchronous oscillations for $\Omega = 0.5$, $\varepsilon = 0.3$, $\omega = 1$ and different I . (a) in coordinates x, y ; (b) in the stereographic projection.

Our next goal is to establish stability of this periodic regime with respect to synchrony breaking. Starting with the synchronous solution of system (7), we look what happens if just one element of the array slightly deviates from this solution. This means that we perturb $\theta \rightarrow \theta^0 + \delta\theta$, $\phi \rightarrow \phi^0 + \delta\phi$, while keeping the mean field X and the global variables u, w at their values on the limit cycle (we do not write index at θ, ϕ here because any oscillator can be perturbed, equations for the variations do not depend on the index). As a result, we get a two-dimensional linear system for $(\delta\phi, \delta\theta)$ with T -periodic coefficients determined by $(\theta^0(t), \phi^0(t), u^0(t), w^0(t))$. Solutions of such a Mathieu-type system are functions $\Theta_{1,2}(t) \exp(\lambda_{1,2}t)$, $\Phi_{1,2}(t) \exp(\lambda_{1,2}t)$ where $\Theta_{1,2}(t) = \Theta_{1,2}(t + T)$, $\Phi_{1,2}(t) = \Phi_{1,2}(t + T)$ are T -periodic. The resulting stability is determined by multipliers $\mu_{1,2} = \exp[\lambda_{1,2}T]$: the perturbation $(\delta\phi, \delta\theta)$ decays if $|\mu_{1,2}| < 1$ and increases otherwise. The calculation of this evaporation multiplier²⁹ thus allows us to characterize linear stability of the synchronous cluster.

The calculation of the evaporation multipliers is a straightforward numerical task after the periodic solution $(\theta^0(t), \phi^0(t), u^0(t), w^0(t))$ is found, we illustrate in Fig. 4 the stability region on plane of parameters (ω, I) . The smaller values of the largest evaporation multiplier correspond to stronger stability of synchrony and to more robust synchronization. In numerical simulations for $\omega = 1$, we observed that the complete synchrony establishes for $0.009 \lesssim I$: in all performed runs with $N = 200$ starting from random initial conditions,

either the full synchrony was established, or at the end of calculations a large cluster with almost all synchronous oscillators was observed, plus at most one or two that still did not belong to this majority cluster. This parameter range can be thus characterized as that of robust complete synchrony. For $I \lesssim 0.009$, although there is a region where the complete synchrony is stable, it does not typically evolve from the random initial conditions, as outlined below.

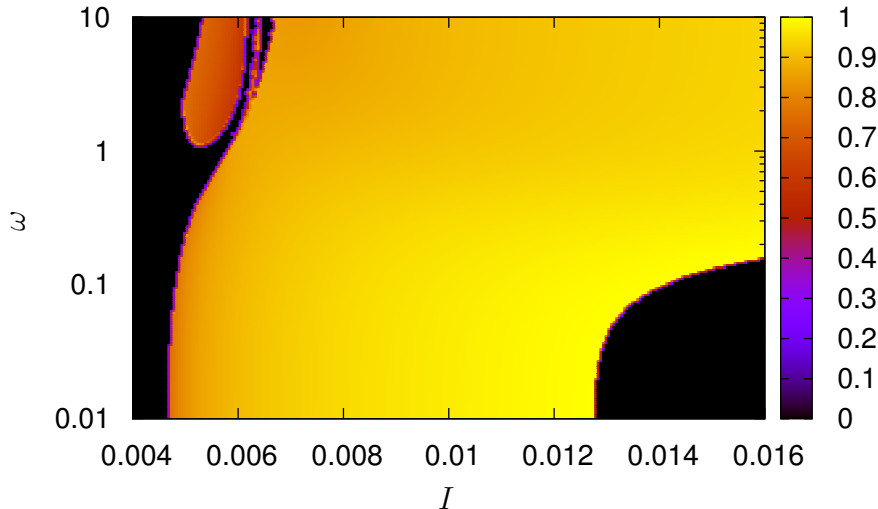


FIG. 4. (color online) Stability region for $\Omega = 0.5$, $\varepsilon = 0.3$: Instability is shown by black; otherwise color represents the absolute value of the largest evaporation multiplier.

B. Clusters

The systematic study of all possible cluster states is hardly possible, so we restricted our attention to two types of numerical experiments. In the first one, a statistical analysis of possible cluster states in the array of STOs has been performed. The simulations in the array of 200 oscillators with $\Omega = 0.5$, $\varepsilon = 0.3$, $\omega = 1$ have been started from random initial conditions, and the final state after the transient $t = 10^5$ has been analyzed. For $0.004 \leq I \leq 0.005$ no formation of large clusters have been observed. For $I = 0.004$ typically all oscillators remain different, in few cases a small number of clusters of size 2 is built. For $I = 0.005$ building of many small clusters is typical, and clusters with sizes up to 37 have been observed. For $I = 0.006$ typically two-cluster states develop, but in 0.4% of all runs no essential clustering have been observed. For larger currents, $I \geq 0.007$, clustering

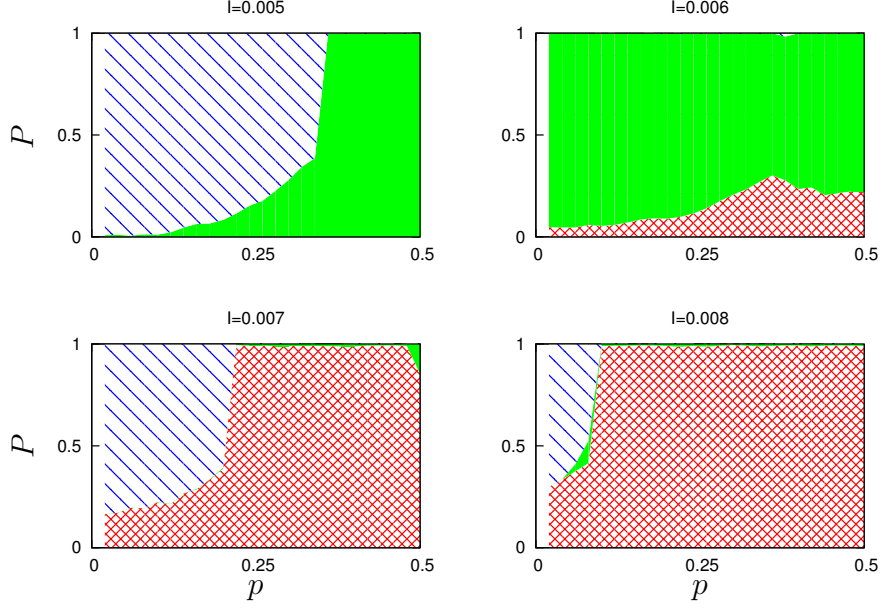


FIG. 5. (color online) Statistical evaluation of the evolution of initially randomly initialized 2-cluster state: probability P to observe different states vs. cluster distribution p , for several values of parameter I . Patterns from bottom to top depict regimes of one cluster (red, crossed pattern), 2 clusters with periodic dynamics (green, filled pattern), and 2 clusters with complex dynamics (mostly quasiperiodic, blue, inclined lines).

was always observed. For $0.007 \leq I \leq 0.008$ in many cases it was not complete: together with a large cluster, a set of non-clustered oscillators exists at the end of the transient time; for $0.009 \leq I \leq 0.014$ clustering was always a full one, with typically all oscillators fully synchronized (1-cluster state).

In the second numerical experiment we initially prepared a 2-cluster state, with a given distribution p between clusters ($p = N_1/N$, where N_1 is the number of oscillators in the first cluster). This 2-cluster state has been followed in time to see, if the clusters remain separated or they merge to 1-cluster (complete synchrony). The results are shown in Fig. 5. In the range $0.009 \leq I \leq 0.014$ practically all initial configurations eventually resulted in complete synchrony (not shown). For $I = 0.004, 0.005$ no one merging event has been observed; this corresponds to the fact that 1-cluster state is unstable for these parameters, as described above. For $0.006 \leq I \leq 0.008$ both 2-cluster and 1-cluster states are observed. For $I = 0.007, 0.008$ the 2-cluster states prevail for small p , i.e. for very asymmetric distribution among the clusters, here the regime is typically quasiperiodic. For $I = 0.006$ the 2-cluster

state is usually periodic, and there is a finite probability to merge. We illustrate a cluster state with a quasiperiodic mean field in Fig. 6.

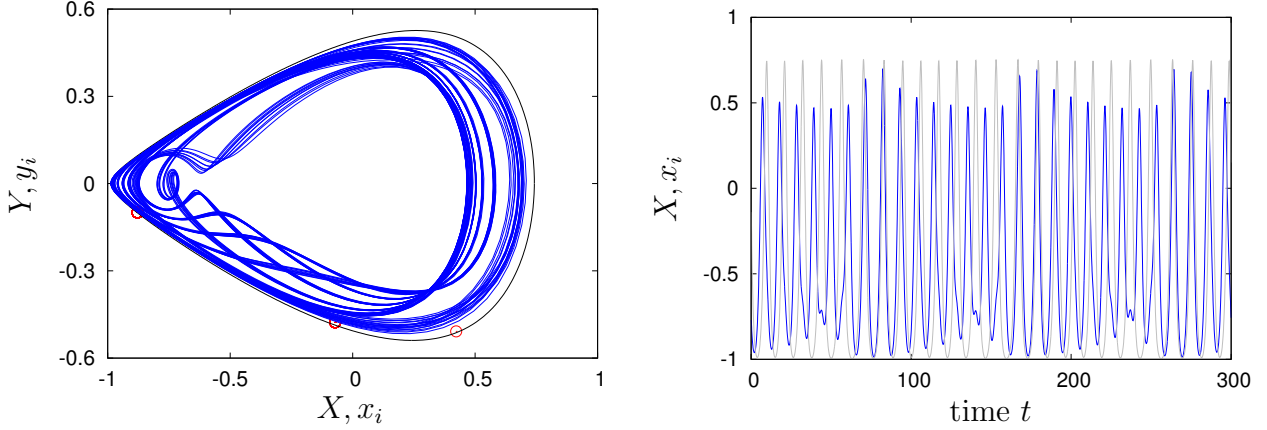


FIG. 6. (color online) A clustered regime for $I = 0.007$. The array with $N = 200$ builds 2 clusters with $N_1 = 168$, $N_2 = 31$ and one separated oscillator. Left panel: a cluster state (red circles) and the evolution of the mean field (blue curve) in coordinates X, x_i vs Y, y_i . Black line shows for comparison the fully synchronous regime for these parameters. Right panel: the mean field $X(t)$ (blue curve) and the oscillations of one of the oscillators (grey curve).

C. Asynchronous state

In this state, which is observed for $I \lesssim 0.0045$, the oscillators are uniformly (in time) distributed over the limit cycle, while the mean field vanishes. We illustrate this regime in Fig. 7.

D. Partial synchrony

Regimes of partial synchrony, with a large number of clusters and non-vanishing mean field (which is nevertheless definitely smaller than in the case of full synchrony) are observed in the range $0.0045 \lesssim I \lesssim 0.006$. Typically these states are chaotic, as illustrated in Fig. 8. However, one cannot exclude that such a state is in fact a very long transient, and asymptotically for long times the clusters will “grow”.

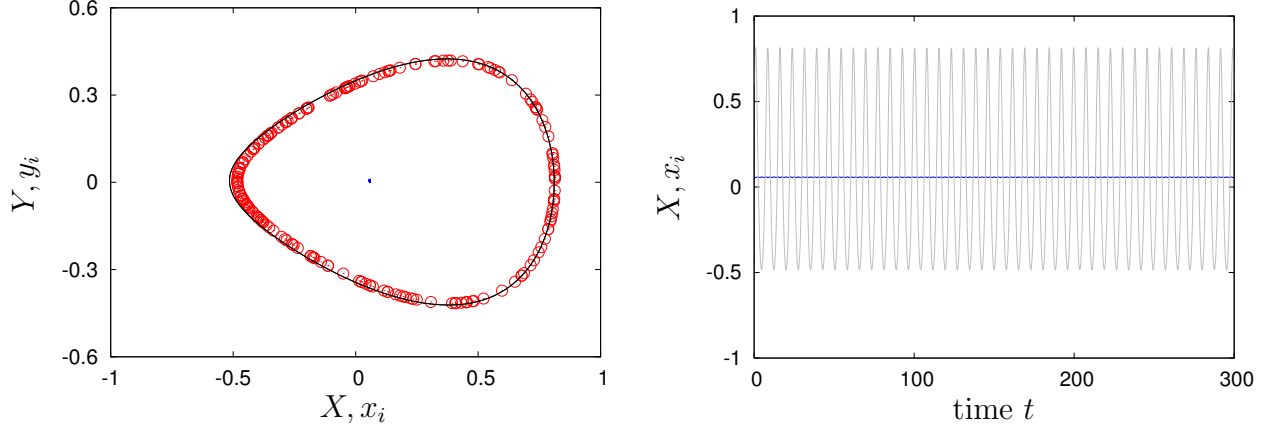


FIG. 7. (color online) An asynchronous regime for $I = 0.004$. Left panel: snapshot (red circles) of the state and the evolution of the mean field (blue curve, hardly seen at the origin) in coordinates X, x_i vs Y, y_i . Black line shows for comparison the fully synchronous regime for these parameters. Right panel: the mean field $X(t)$ (blue curve) and the oscillations of one of the oscillators (grey curve).

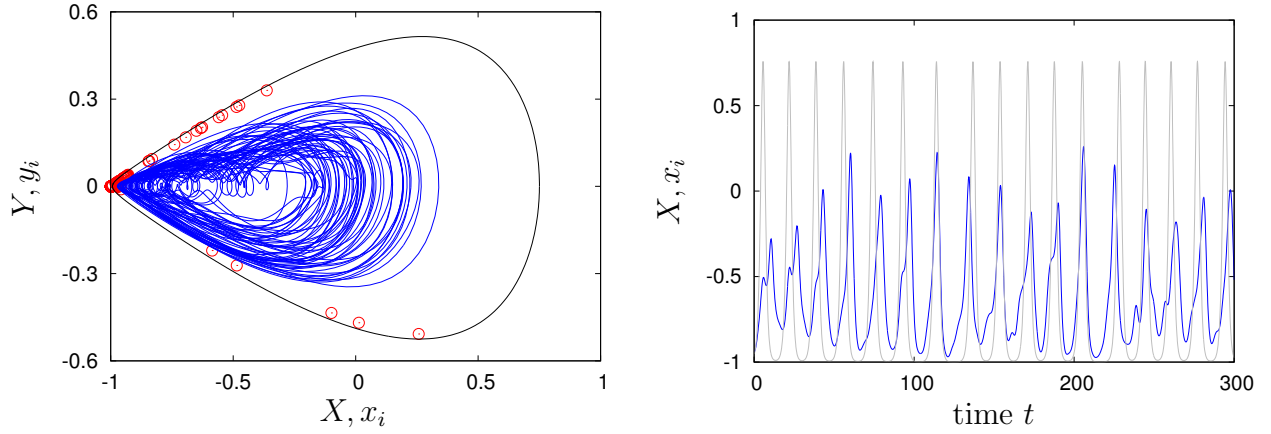


FIG. 8. (color online) A partially synchronous regime with chaotic mean field for $I = 0.006$. Left panel: snapshot (red circles) of the state and the evolution of the mean field (blue curve) in coordinates X, x_i vs Y, y_i . Black line shows for comparison the fully synchronous regime for these parameters. Right panel: the mean field $X(t)$ (blue curve) and the oscillations of one of the oscillators (grey curve).

IV. CONCLUSION

In this paper we have considered an array of spin-torque oscillators with a parallel inductor-capacitor-resistor load, and demonstrated that in this setup a robust synchronization regime is observed in a wide range of parameters. While the region of stability of the synchronous regime is large, not always one observes full synchrony inside this domain: often oscillators organize themselves in several clusters, so that the synchrony is only partial. Transition from asynchronous state to partial and full synchrony is rather nontrivial, with chaotic and quasiperiodic regimes of the mean field. These particular properties of the STO oscillators make an application of simple models like that of Kuramoto model of phase coupled oscillators questionable.

We have focused on the simplest setup, where all the oscillators are identical. To make realistic predictions, one has to take into account diversity of oscillator parameters (and, possibly, fluctuations); however the range of parameters (especially of that of the load) mostly promising for maximal synchrony can be estimated from the study of identical oscillators, as the region of maximal stability of the synchronous state and of absence of clustering. Remarkably, this stability can be determined in a rather simple way, by calculating the evaporation exponent of the synchronous 1-cluster state as described in Sect. III A. One can easily adopt this method to other sets of parameters, and to other types of load. Another possible extension of this study is consideration of coupling schemes beyond the globally coupled ones, similar to the corresponding studies of one-dimensional Josephson junction arrays³⁰; here however methods developed for global coupling cannot be directly applied.

ACKNOWLEDGMENTS

The authors thanks NEXT program for support, IRSAMC for hospitality, and D. Shepelyansky and M. Rosenblum for helpful discussions.

Appendix A: Equations in dimensionless form

We combine together Eqs. (1,3,4,5,6):

$$\begin{aligned}
\frac{1+\alpha^2}{\gamma}\dot{\theta}_i &= U \cos \theta_i \cos \phi_i - W \sin \phi_i + \alpha S - T \\
\frac{1+\alpha^2}{\gamma}\sin \theta_i \dot{\phi}_i &= -U \sin \phi_i - W \cos \phi_i \cos \theta_i - S - \alpha T \\
S &= (H_{dz} + H_k \cos^2 \phi_i) \sin \theta_i \cos \theta_i \quad T = H_k \sin \phi_i \cos \phi_i \sin \theta_i \\
U &= \alpha H_a - \beta(I - C \frac{dV}{dt}) \quad W = H_a + \alpha \beta(I - C \frac{dV}{dt}) \\
LC \frac{d^2 V}{dt^2} + rC \frac{dV}{dt} + V &= NR_0(1 - \varepsilon X)(I - C \frac{dV}{dt})
\end{aligned} \tag{A1}$$

We introduce new time $t' = \frac{\gamma}{1+\alpha^2}t$ and dimensionless voltage $v = \frac{V}{R_0 I}$, and obtain, denoting $\frac{\gamma^2}{(1+\alpha^2)^2}LC = \Omega^{-2}$ and $\frac{NR_0 C \gamma}{1+\alpha^2} = \omega^{-1}$

$$\begin{aligned}
\dot{\theta}_i &= U \cos \theta_i \cos \phi_i - W \sin \phi_i + \alpha S - T \\
\sin \theta_i \dot{\phi}_i &= -U \sin \phi_i - W \cos \phi_i \cos \theta_i - S - \alpha T \\
S &= (H_{dz} + H_k \cos^2 \phi_i) \sin \theta_i \cos \theta_i \quad T = H_k \sin \phi_i \cos \phi_i \sin \theta_i \\
U &= \alpha H_a - \beta I(1 - \frac{1}{N\omega} \frac{dv}{dt}) \quad W = H_a + \alpha \beta I(1 - \frac{1}{N\omega} \frac{dv}{dt}) \\
\frac{1}{\Omega^2} \frac{d^2 v}{dt^2} + \frac{r}{R_0} \frac{1}{N\omega} \frac{dv}{dt} + v &= N(1 - \varepsilon X)(1 - \frac{1}{N\omega} \frac{dv}{dt})
\end{aligned} \tag{A2}$$

Finally, introducing $v = Nu$ and $w = \frac{1}{\omega} \frac{du}{dt}$ we obtain system (7). Additional parameters, related to the load, are: Ω , ω , and $r/(NR_0)$. The latter parameter can be set to zero if the resistance of the load is much smaller than that of the STO array.

¹ A. Slavin and V. Tiberkevich, IEEE T. Magn. **45**, 1875 (2009).

² J. C. Slonczewski, J. Magn. Mater. **159**, L1 (1996).

³ L. Berger, Phys. Rev. B **54**, 9353 (1996).

⁴ S. I. Kiselev, J. C. Sankey, I. N. Krivorotov, N. C. Emley, R. J. Schoelkopf, R. A. Buhrman, and D. C. Ralph, Nature **425**, 380 (2003).

⁵ W. H. Rippard, M. R. Pufall, S. Kaka, S. E. Russek, and T. J. Silva, Phys. Rev. Lett. **92**, 027201 (2004).

- ⁶ A. Pikovsky, M. Rosenblum, and J. Kurths, *Synchronization. A Universal Concept in Nonlinear Sciences*. (Cambridge University Press, Cambridge, 2001).
- ⁷ B. Georges, J. Grollier, M. Darques, V. Cros, C. Deranlot, B. Marcilhac, G. Faini, and A. Fert, Phys. Rev. Lett. **101**, 017201 (2008).
- ⁸ J. Grollier, V. Cros, and A. Fert, Phys. Rev. B **73**, 060409(R) (2006).
- ⁹ B. Georges, J. Grollier, V. Cros, and A. Fert, Applied Physics Letters **92**, 232504 (2008).
- ¹⁰ D. Li, Y. Zhou, C. Zhou, and B. Hu, Phys. Rev. B **82**, 140407 (2010).
- ¹¹ D. Li, Y. Zhou, B. Hu, and C. Zhou, Phys. Rev. B **84**, 104414 (2011).
- ¹² D. Li, Y. Zhou, B. Hu, J. Åkerman, and C. Zhou, Phys. Rev. B **86**, 014418 (2012).
- ¹³ S. Kaka, M. Pufall, W. Rippard, T. Silva, S. Russek, and J. Katine, Nature **437**, 389 (2005).
- ¹⁴ F. B. Mancoff, N. D. Rizzo, B. N. Engel, and S. Tehrani, Nature **437**, 393 (2005).
- ¹⁵ Y. Kuramoto, *Chemical Oscillations, Waves and Turbulence* (Springer, Berlin, 1984).
- ¹⁶ J. A. Acebrón, L. L. Bonilla, C. J. P. Vicente, F. Ritort, and R. Spigler, Rev. Mod. Phys. **77**, 137 (2005).
- ¹⁷ A. N. Slavin and V. S. Tiberkevich, Phys. Rev. B **74**, 104401 (2006).
- ¹⁸ M. Quinsat, V. Tiberkevich, D. Gusakova, A. Slavin, J. F. Sierra, U. Ebels, L. D. Buda-Prejbeanu, B. Dieny, M.-C. Cyrille, A. Zelster, and J. A. Katine, Phys. Rev. B **86**, 104418 (2012).
- ¹⁹ Y. Zhou, V. Tiberkevich, G. Consolo, E. Iacocca, B. Azzerboni, A. Slavin, and J. Åkerman, Phys. Rev. B **82**, 012408 (2010).
- ²⁰ K. Wiesenfeld and J. W. Swift, Phys. Rev. E **51**, 1020 (1995).
- ²¹ K. Wiesenfeld, P. Colet, and S. Strogatz, Physical Review E **57**, 1563 (1998).
- ²² G. Filatrella, N. F. Pedersen, and K. Wiesenfeld, Phys. Rev. E **61**, 2513 (2000).
- ²³ P. Barbara, A. B. Cawthorne, S. V. Shitov, and C. J. Lobb, Phys. Rev. Lett. **82**, 1963 (1999).
- ²⁴ P. Mohanty and A. Politi, J. Phys. A: Math. Gen. **39**, L415 (2006).
- ²⁵ A. Pikovsky and M. Rosenblum, Physica D **238**(1), 27 (2009).
- ²⁶ C. van Vreeswijk, Phys. Rev. E **54**, 5522 (1996).
- ²⁷ V. Hakim and W. J. Rappel, Phys. Rev. A **46**, R7347 (1992).
- ²⁸ N. Nakagawa and Y. Kuramoto, Physica D **75**, 74 (1994).
- ²⁹ A. Pikovsky, O. Popovych, and Y. Maistrenko, Phys. Rev. Lett. **87**, 044102 (2001).
- ³⁰ B. Vasilic, E. Ott, T. Antonsen, P. Barbara, and C. J. Lobb, Phys. Rev. B **68**, 024521 (2003).